Pramana – J. Phys. (2017) 88: 78
DOI 10.1007/s12043-017-1377-0

Fullerene as alligator clips for electrical conduction through anthracene molecular junctions

RUPAN PREET KAUR*, RAVINDER SINGH SAWHNEY and DERICK ENGLES

Department of Electronics Technology, Guru Nanak Dev University, Amritsar 143 001, India
*Corresponding author. E-mail: bhullar.rupan@gmail.com

MS received 10 February 2016; revised 14 November 2016; accepted 16 December 2016; published online 20 April 2017

Abstract. The conductance of a single molecule transport junction comprising anthracene molecular junction (AMJ) with fullerene as alligator clips was investigated using *ab-initio* density functional theory (DFT) in the Landauer–Imry regime of coherent tunnelling transport. In our previous research, we have already calculated the electrical transport properties of aromatic molecules with thiol, amine, hydroxyl and selenol end groups concluding the exceptional assistance in the formation of robust molecular junctions. In this article, we have presented the suitability of fullerene anchoring in coupling anthracene molecule with gold electrodes. AMJ with boron-20 (B-20) and C-20 alligator clips exhibited strongest conduction in contrast to nitrogen, oxygen, fluorine and neon alligator clips.

Keywords. HOMO; LUMO; fullerenes; alligator clips; eigenstates; molecular energy spectrum; hybridization; coupling; tunnelling.

PACS Nos 85.35.−p; 85.65.−h; 73.23.−b; 73.40.−c

1. Introduction

The measurement and understanding of electron transport through a single molecule electrically connected to two metallic electrodes is an essential step in the development of molecular electronics [1,2]. Compared to saturated molecules like alkanes, conjugated molecules are more suitable for potential applications in molecular electronic devices due to their small HOMO–LUMO gap (HLG) [3]. The electrical conducting properties of benzene (a typical aromatic molecule) with thiol and amine alligator clips have been extensively studied by various researchers and the conduction was far from perfect, the reason being the lack of an efficient conducting channel at the Au–S contact and the Au–N contact [4,5]. Martin *et al* [6] proposed the idea of using fullerene as alligator clips in forming molecular junctions instead of thiol or amine groups. Their work concluded the better stability of fullerene–gold surfaces leading to strong hybridization of molecule with gold electrodes. Therefore, in order to observe the increased conduction of a molecular junction formed by fullerene alligator clips, we considered anthracene, a polyaromatic molecule sandwiched between two gold electrodes with interface being X-20 fullerene, where X represents boron, carbon, nitrogen, oxygen, fluorine and neon atoms.

Fullerenes are known to hybridize strongly with gold surfaces [7] which can be treated as 'effective electrodes' leading to charge injection into the molecular core [8]. This study was done by taking the most distinguished work by Martin *et al* [6] as reference, which was based on C-60 fullerenes as alligator clips, and extending the same for X-20 fullerene anchors, X being atoms ranging from boron to neon of the second period of the periodic table. By deploying fullerenes as anchors, we achieved definite proliferation in conduction by some orders of quanta.

2. Computational model

The two-probe model in this study consisted of left and right semi-infinite gold electrodes that act as the source and the drain of a conventional transistor and the scattering region constituting the molecule anthracene with fullerene B-20 as alligator clips in the first case followed by C-20, N-20, O-20, F-20 and

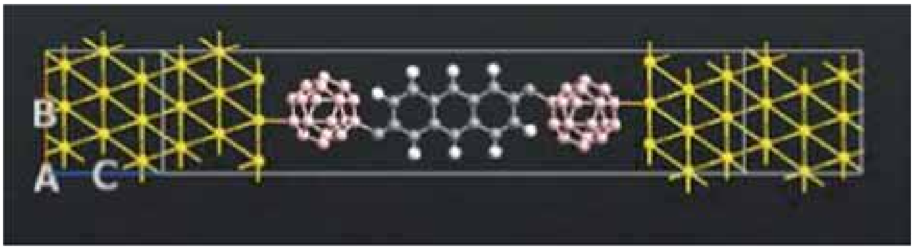

Figure 1. Molecular junction comprising bis-fullero (C-20) anthracene molecule sandwiched between two gold electrodes.

Ne-20. Molecular junction comprising bis-fullero (C-20) anthracene molecule sandwiched between two gold electrodes is shown in figure 1. This arrangement can be represented as 'bis-fullero anthracene' molecule. Clusters of atoms from gold were added to the ends of the scattering region to form an 'extended molecule', which was further connected to additional atoms of the gold electrodes. The AMJs formed were modelled using quantum-wise Atomistic Toolkit ATK 13.8.0 [9] and its graphical user interface Virtual Nanolab [10] based on *ab-initio* density functional theory in combination with non-equilibrium Green's function (DFT+NEGF) approach. The results are represented in the form of $I-V$ curves, conductance–voltage curves, device density of states, transmission spectrum, molecular energy spectrum and molecular projected self-consistent Hamiltonian (MPSH) eigenstates under bias voltages ranging from -2 V to $+2$ V with a step size of 0.4.

The coupling between the molecule and the gold electrodes can be represented using Green's function approach as [11]

$$G(E) = 1/[ES - F - \Sigma_{\mathrm{L}}(E) - \Sigma_{\mathrm{R}}(E)], \quad (1)$$

where S is the overlap matrix, F is the Fock matrix of the extended molecule (EM) and $\Sigma_{\mathrm{L}}(E)$, $\Sigma_{\mathrm{R}}(E)$

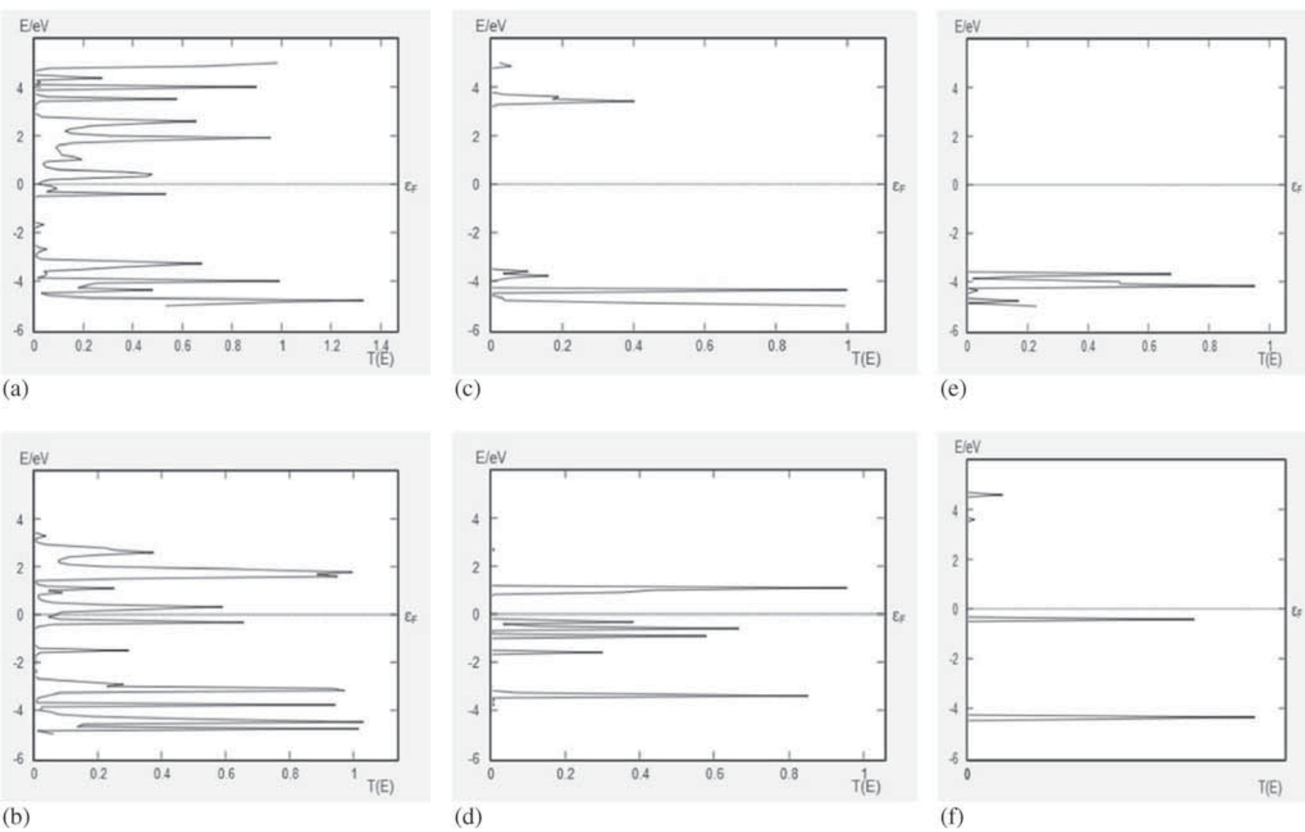

Figure 2. Equilibrium transmission spectra of AMJs comprising anthracene molecule stringed to gold electrodes via (**a**) B-20, (**b**) C-20, (**c**) N-20, (**d**) O-2, (**e**) F-20 and (**f**) Ne-20 as alligator clips.

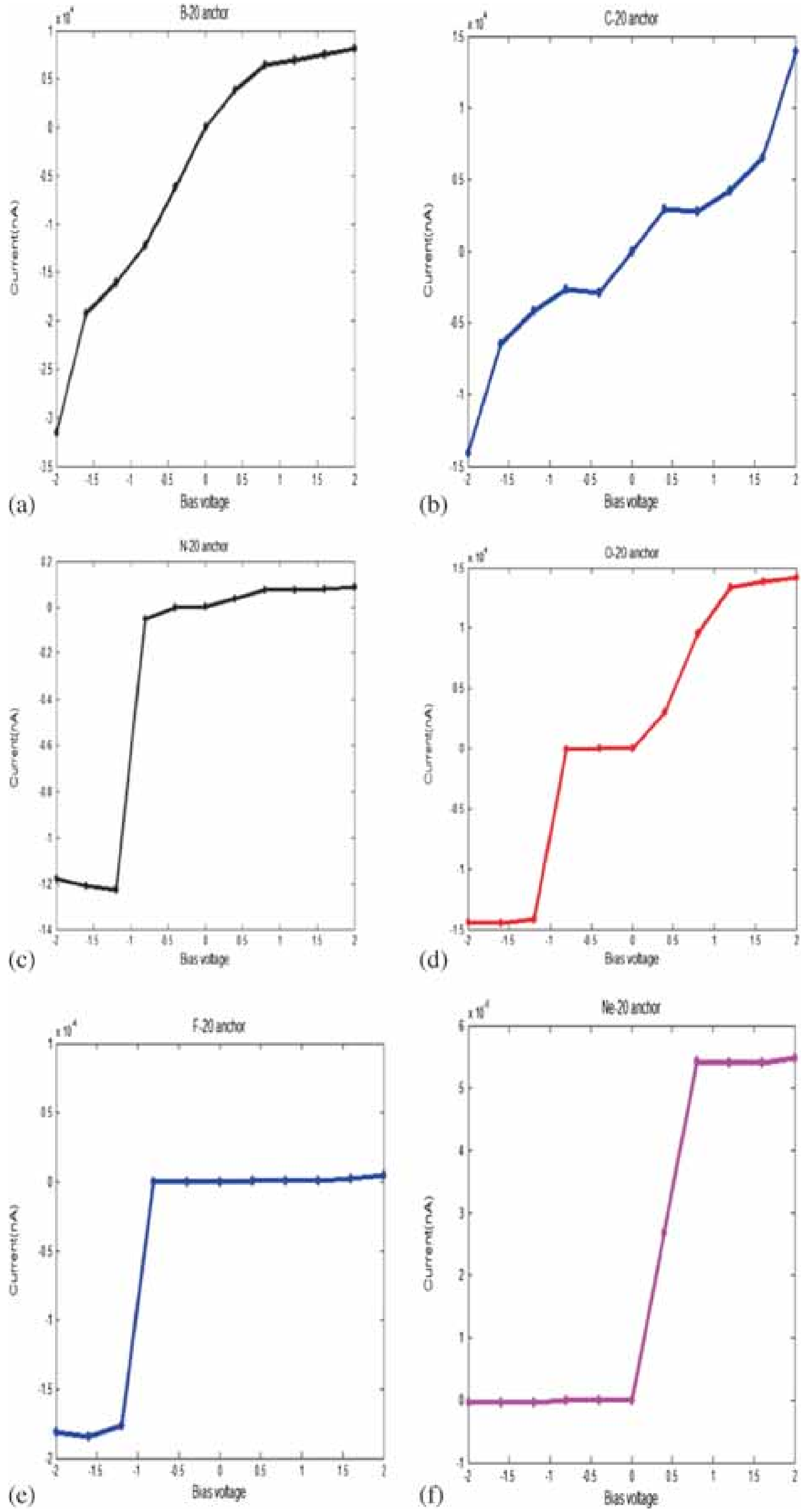

Figure 3. $I-V$ curves by different alligator clips [starting from B-20 (**a**) to Ne-20 (**f**)].

are self-energies that define coupling of ADT with the contacts.

$$\Sigma(E) = \Gamma^T g_s(E)\Gamma, \quad (2)$$

where Γ is a matrix that gives couplings between the extended molecule and atoms in the contacts and $g_s(E)$ is a matrix representing the surface Green's function for a semi-infinite bulk metal. In addition to geometrical and electrical information about the contacts, self-energy also defines the strength of coupling between the molecule and electrodes because it is responsible for the shifting and broadening of molecular energy levels.

3. Results and discussions

We have employed density functional theory (DFT) combined within Keldysh NEGF framework [12] to compute the conductance of the modelled AMJs. Optimum length of electrodes was taken as 7 Å and the Brillouin zone was sampled with 1*1*100 points depict A, B and C directions as depicted in model of figure 1. All the calculations were performed with a mesh cut-off energy of 100 Hartrees to achieve a balance between the computation time and the accuracy. Once a self-consistent Hamiltonian was obtained, we evaluated the transmission function using the Landauer relation [13] given below:

$$T^k(E,V) = \mathrm{Tr}[\Gamma_1^k(E,V)G_M^k(E,V) \times \Gamma_2^k(E,V)G_M^{k'}(E,V)], \quad (3)$$

where $\Gamma(E)$ is the coupling function that gives information about the quality of the contact between the molecule and the electrodes as well as information about the density of states in the bulk available for current transmission across the junction. From figure 2, we can see that B-20 exhibits the maximum number of transmission states, followed by C-20, further followed by O-20. N-20, F-20, and Ne-20 exhibits negligible transmissions. The interface between metal electrodes and molecule is of paramount importance for the transport of electron through single molecule [14], and here C-20 provides the strongest interface between π-electron cloud of anthracene ring and gold electrodes whereas Ne-20, being the most inert, proved to be the weakest interface followed by halogen F-20, N-20 and chalcogen O-20.

$I-V$ curves were obtained by integrating the transmission spectra for distinct values of bias ranging from -2 V to $+2$ V. Current and conductance values were calculated from the transmission coefficient $T(E)$ using the following equation:

$$I = \frac{2e}{h}\int_{-\infty}^{\infty} T(E,V_b)[f(E-\mu_L) - f(E-\mu_R)]\mathrm{d}E \quad (4)$$

in an energy window of width V_b around the Fermi energy E_f, $\mu_{L/R}$ is the electrochemical potential applied at the left or the right electrode, e/h is the current per mode per energy.

Figures 3a–3f show the current–voltage curves exhibited by different alligator clips. As expected from the transmission spectra of AMJs, the values of current also followed the same analogous order displaying maximum current by B-20 and C-20 and least by Ne-20. Since B-20 and C-20 exhibited maximum current, we further compared their $I-V$ curves in figure 4. B-20 exhibited higher current during both forward as well as reverse bias voltages except at the highest bias point i.e. +2 V, where C-20 attained its maxima. Highest current reported by B-20 proved its metallic character and hence its stronger coupling with gold electrode atoms whereas lowest current by Ne-20 justified its non-metallic nature. Strong coupling of molecules with the surface of the electrode leads to direct tunnelling of electrons through the molecule whereas weak coupling makes it a two-step process where electrons reside in the molecule as some electrons move from the source to the drain electrode. This weak coupled transport is labelled as 'Coulomb blockade' [15], which can be referred to as AMJ comprising Ne-20, F-20, N-20 and O-20 alligator clips.

In order to further investigate the conduction behaviour of AMJs, their values of conductance were

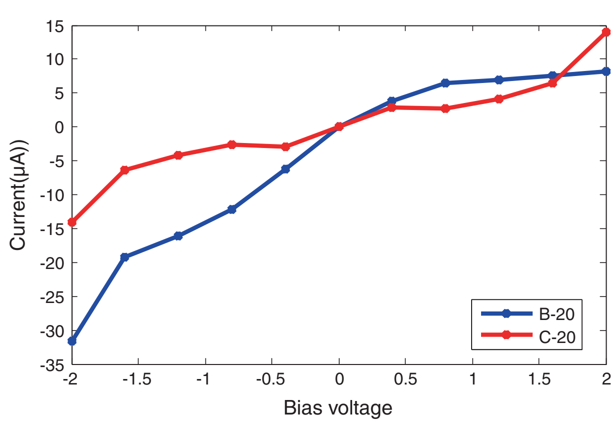

Figure 4. Comparison of $I-V$ curves between B-20 and C-20 as alligator clips of AMJ.

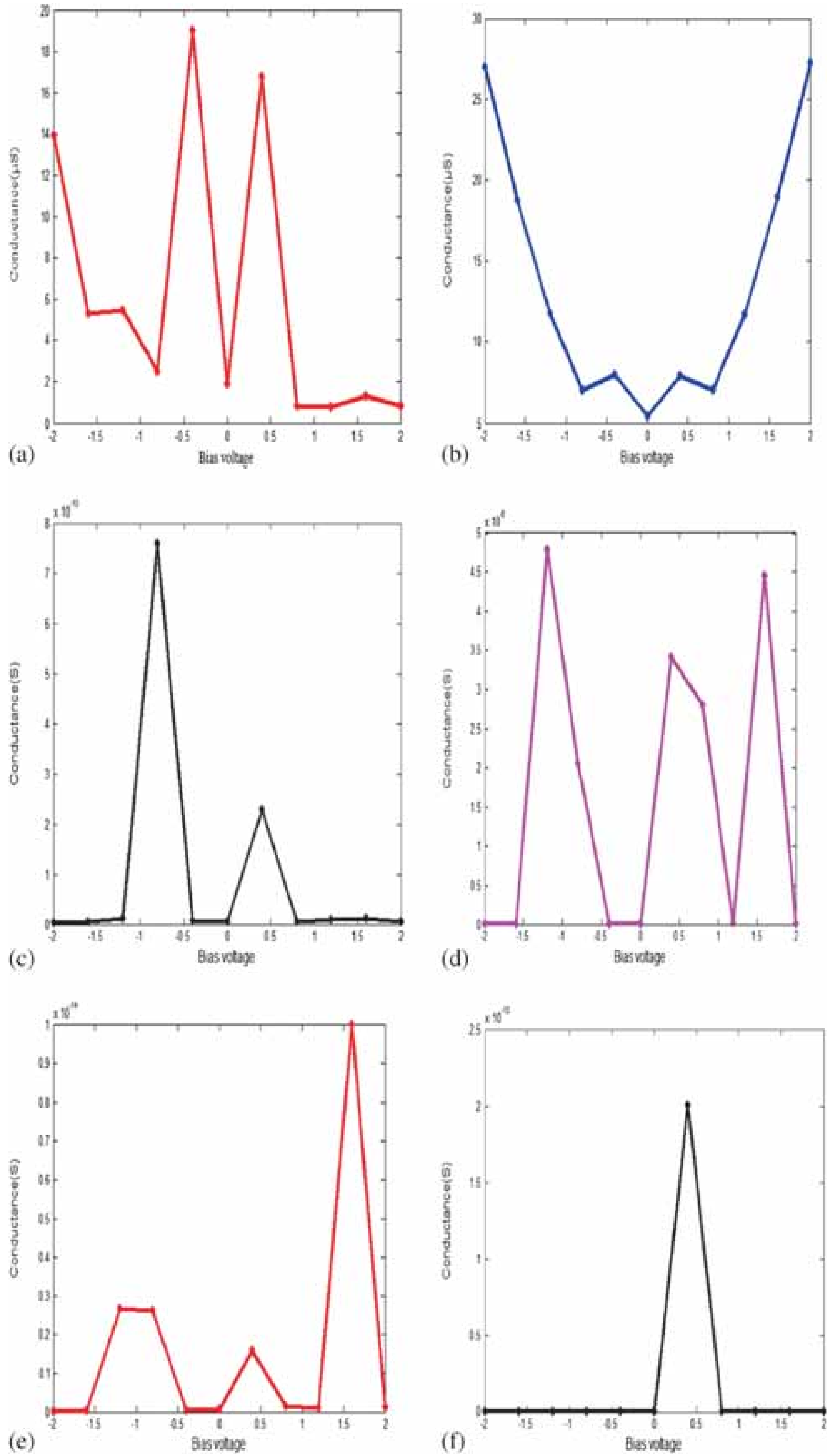

Figure 5. Conductance (S)–bias voltage (V) curves exhibited by AMJs with (**a**) B-20, (**b**) C-20, (**c**) N-20, (**d**) O-20, (**e**) F-20 and (**f**) Ne-20 as alligator clips.

computed with the help of expression (5) and shown in figure 5.

$$G = T(E_F)G_0, \tag{5}$$

where $G_0 = 2e^2/h$ is the quantum of conductance.

The corresponding G–V (conductance–bias voltage) curves also exhibit similar order justified by the transmission spectra at zero bias and current–voltage curves except the conduction displayed by B-20 and C-20, which are further compared in figure 6.

From figure 6, we can see that C-20 alligator clips exhibit higher conductance than B-20 clips except at two bias points +/− 0.4 V. B-20 clips exhibit two symmetrical maxima (0.24 and 0.22 quanta of conductance respectively) at +/−0.4 V around zero bias voltage. In contrast to B-20 clips, C-20 clips also exhibit two symmetrical maxima of approximately the same value ($0.35G_0$) at +/−2 V around zero bias voltage. Conduction exhibited by all alligator clips under study could be justified by their transmission spectra (explained in figure 2) and HOMO–LUMO gap exhibited by AMJs. Hence, we computed HLG of these clips and plotted in figure 7, where we observe that the highest HLG is for Ne-20 followed by F-20, further followed by N-20 and O-20 whereas least HLG is exhibited by C-20 followed by B-20. Similar G–V behaviour can be seen in figure 5.

We further studied the transmission spectra at −/+ 0.4 V for B-20 alligator clips and figure 8 shows transmission coefficient $T(E)$ exhibited by B-20 as a function of energy (eV) at −0.4 V and +0.4 V. Here, we observed similarity in the transmission peaks at different energy levels except that $T(E)$ at −0.4 V is higher in comparison to that at +0.4 V. Similarly, +/− 2 V and 0 V were the values of interest of $T(E)$ for C-20 reported in figure 9, where we observed same values are exhibited by AMJ at +/−2 V because of

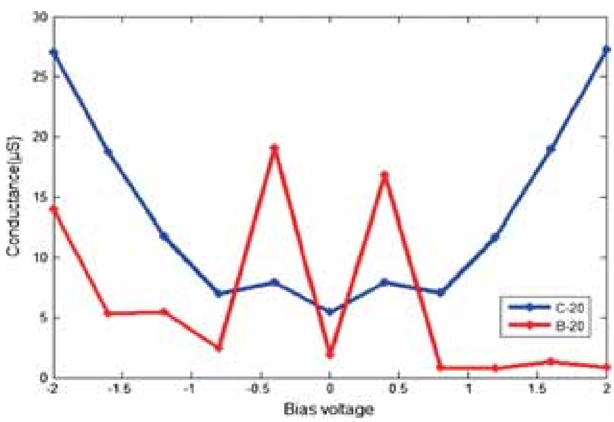

Figure 6. Conductance (μS)–bias voltage (V) comparison between B-20 and C-20 as alligator clips of AMJ.

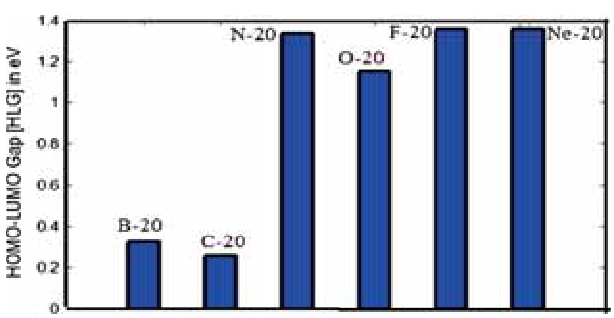

Figure 7. HOMO–LUMO gap (eV) exhibited by B-20, C-20, N-20, O-20, F-20 and Ne-20 as alligator clips at zero bias voltage.

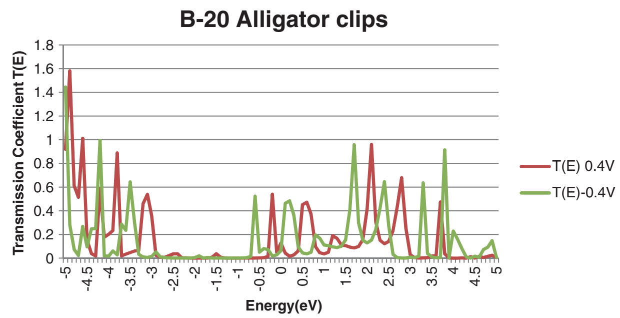

Figure 8. Transmission coefficient $T(E)$ exhibited by B-20 as a function of energy (eV) at −0.4 V and +0.4 V where $T(E)$ at −0.4 V was found to be a little bit higher than that at +0.4 V.

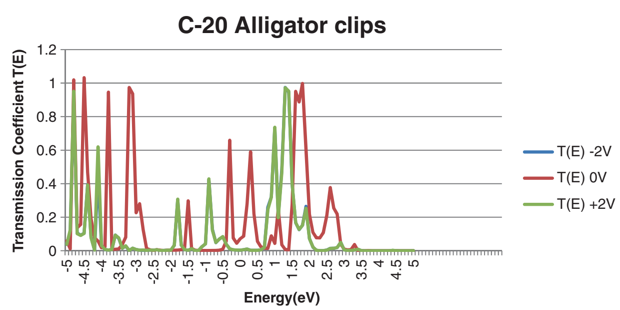

Figure 9. Transmission coefficient $T(E)$ exhibited by C-20 as a function of energy (eV) at −2 V, 0 V and +2 V where $T(E)$ at −2 V and +2 V exhibited approximately the same value because of which the curves were found to coincide.

Table 1. Values of HOMO, LUMO and HLG at +2 V.

Energy levels (eV)	B-20 Alligator clips	C-20 Alligator clips
HOMO	−0.4914	−0.532
LUMO	0.5918	0.151
HLG	1.0832	0.683

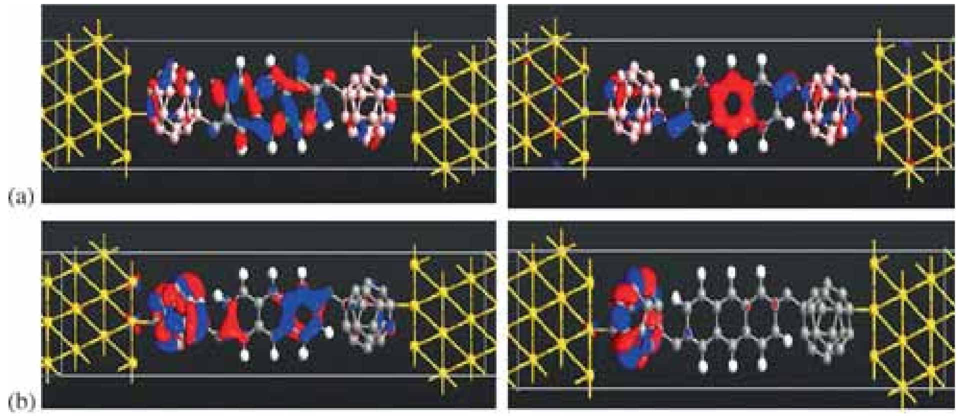

Figure 10. MPSH eigenstates exhibited by (**a**) B-20 alligator clips and (**b**) C-20 alligator clips where we found prominent delocalization of electron cloud at left C-20 alligator clip of AMJ whereas AMJ with B-20 alligator clips exhibited delocalization around anthracene ring rather than B-20 around alligator clips.

which their conductance came out to be equal, i.e. 0.35 quanta of conductance.

High conductance exhibited by C-20 alligator clips at the highest bias voltage +2 V was further explored by studying its molecular energy levels where we found that it has 0.683 eV HOMO–LUMO gap (HLG) in contrast to 1.0832 eV exhibited by B-20 alligator clips. When HLG is smaller, the corresponding work function will be smaller to overcome the HLG, resulting in more transmissions as seen in figure 8 and table 1. On the other hand, B-20 alligator clips have larger HLG because of which large work function was required and hence difficulty in exhibiting transmission of electrons [16] and hence lower $T(E)$ at +2 V. In addition to their energy levels, we also explored their corresponding eigenstates at +2 V, shown in figures 9a and 9b. Figures 10a and 10b outline the localization and delocalization of electrons around the extended molecule for B-20 and C-20 alligator clips respectively. Comparing these figures, we can clearly distinguish different roles of alligator clips in transmissions. More the delocalization of electron cloud around the molecule, more are the transmissions and hence higher is the conduction and the same can be observed for C-20 alligator clips. Left C-20 alligator clip exhibited prominent role in conduction in comparison to right one as the former displayed prominent delocalization of electrons [17] around the C-20 fullerene molecule. Moreover, HOMO opened stronger conducting channel which is responsible for the highest conduction of C-20 alligator clips at +2 V.

4. Conclusions

DFT method combined with NEGF framework was employed to investigate the influence of fullerene-20 as interface between anthracene moiety and gold electrodes. Six different test beds were modelled and their results concluded B-20 and C-20 fullerenes as potential alligator clips to proliferate the conduction of anthracene molecular junctions whereas Ne-20, F-20, N-20 and O-20 showed petite (weak) conduction behaviour. Further, their conducting behaviour was verified by computing their transmission spectra, HLG values and MPSH eigenstates. We firmly believe that these findings can help in developing new molecular structures with better contact between molecule and metal surfaces, an important step towards future development of integrated devices with multiple single molecule components [18,19].

References

[1] A Nitzan and M A Ratner, *Science* **300**, 1384 (2003)
[2] N J Tao, *Nat. Nanotechnol.* **1**, 173 (2006)
[3] Shimin Hou *et al*, *Chem. Phys.* **354**, 106 (2008)
[4] M Siaj and P H McBreen, *Science* **309**, 588 (2005)
[5] C Toher and S Sanvito, *Phys. Rev. Lett.* **99**, 056801 (2007)
[6] C A Martin *et al*, *J. Am. Chem. Soc.* **130**, 13198 (2008)
[7] C Rogero, J I Pascual, J Gómez-Herrero and A M Baró, *J. Chem. Phys.* **116**, 832 (2002)
[8] Y Xue, S Datta and M A Ratner, *J. Chem. Phys.* **115**, 4292 (2001)
[9] Atomistic Toolkit Manual, Quantumwise Inc.
[10] D Kienle, K H Bevan, G-C Liang, L Siddiqui, J I Cerda and A W Ghosh, *J. Appl. Phys.* **100**, 043715 (2006)
[11] John W Lawson and Charles W Bauschlicher Jr, *Phys. Rev. B* **74**, 125401 (2006)
[12] M Brandbyge, J L Mozos, J Taylor and K Stokbro, *Phys. Rev. B* **65**, 165401 (2002)

[13] M Büttiker and R Landauer, *Phys. Rev. B* **31**, 6207 (1985)
[14] K Moth-Poulsen and T Bjørnholm, *Nat. Nanotechnol.* **4**(**9**), 551 (2009)
[15] A V Danilov *et al*, *Nano Lett.* **8**, 1 (2008)
[16] Rupan Preet Kaur, Ravinder Singh Sawhney and Derick Engles, *J. Multiscale Model.* **5**(**2**), 1350009 (2014)
[17] Rupan Preet Kaur, Ravinder Singh Sawhney and Derick Engles, *J. Multiscale Model.* **4**, 1250015 (2012)
[18] T Jain, F Westerlund, E Johnson, K Moth-Poulsen and T Bjørnholm, *ACS Nano* **3**(**4**), 828 (2009)
[19] Q Tang, Y Tong, T Jain, T Hassenkam, Q Wan, K Moth-Poulsen and T Bjørnholm, *Nanotechnology* **20**(**24**), 245205 (2009)